

## Triply-differential cross sections for electron-impact ionization of atomic hydrogen

A. C. Roy

*Department of Physics, University of Kalyani, Kalyani 741 235, West Bengal, India*

A. K. Das and N. C. Sil

*Department of Theoretical Physics, Indian Association for the Cultivation of Science, Jadavpur, Calcutta 700032, India*

(Received 29 April 1980)

A method for obtaining triply-differential cross sections (TDCS) for electron-impact ionization of atomic hydrogen in the Glauber approximation is developed. The expression for the Glauber amplitude in the present case turns out to be a simple two-dimensional integral which can be accurately evaluated. The present procedure has an advantage over the conventional partial-wave technique in calculating TDCS in that the latter requires substantial computer time where many partial waves are involved. We present numerical results for electron-impact ionization of hydrogen atoms at incident energies of 100, 113.6, and 250 eV. A comparison is made of the present TDCS with the corresponding results of the first Born approximation and experiment.

### I. INTRODUCTION

Scattering cross sections for electron-impact ionization of atomic systems are in demand in studies of planetary atmospheres, plasma physics, and radiation physics. In particular, these data are essential in controlled thermonuclear research. To date, a large number of theoretical and experimental investigations have been made on the ionization of atoms by electron impact.<sup>1</sup> These investigations were, until recently, primarily related to the total ionization cross sections. Comparison of total cross sections with the experimental data does not, however, represent an adequate test of theory because important features can be missed in the process of summing and averaging necessary for obtaining total cross sections. So a comparison of cross sections that are differential in one or more kinematic parameters is required for a more definitive test.

Triply-differential cross sections (TDCS) provide the most detailed information on an ionization process. With the report of the first measurements of TDCS on  $e^-$ -He collision by Ehrhardt *et al.*<sup>2</sup> in 1969, considerable interest has grown in the theoretical studies of this phenomenon. Since then, several measurements have been made but they are mostly concerned with complex atoms.<sup>3</sup> The first experimental measurement of TDCS on  $e^-$ -H collision was made by Weigold *et al.*<sup>4,5</sup> They reported the TDCS for coplanar kinematics at incident energies of 100, 113.6, 250, and 413.6 eV for a variety of ejected-electron energies and scattering angles. They compared their data with the corresponding cross sections obtained in the plane-wave Born exchange, plane-wave impulse, and factorized distorted-wave half off-shell impulse approximations. TDCS calculations have also been performed using the first Born approxi-

mation<sup>6</sup> (FBA), the Coulomb-projected Born approximation,<sup>7,8</sup> and the distorted-wave approximation.<sup>9</sup> A comparison of these calculations with experiment has shown that none of these theories can successfully reproduce the experimental results. The distorted-wave model, however, gives a better overall description of the shape of the experimentally observed angular distribution than the Born calculations.

Recently, the Glauber approximation (GA) has been applied with success to a large number of atomic collisions, especially inelastic collisions.<sup>10</sup> More recently, the GA has been applied to the ionization of atomic systems by Thomas,<sup>11</sup> McGuire and co-workers,<sup>12-18</sup> Tsuji *et al.*,<sup>19</sup> and Narumi *et al.*<sup>20</sup>

This paper reports an application of the GA to calculate the TDCS for electron-impact ionization of atomic hydrogen without the use of partial-wave technique and compares the calculated cross sections with the corresponding experimental data of Weigold *et al.* Although McGuire *et al.*<sup>13</sup> and Narumi *et al.* have proposed two different methods for obtaining the Glauber amplitude for the  $H(e, 2e)H^+$  process, there are no reported TDCS calculations using these techniques. Both the approaches are based on partial-wave decomposition of the scattering amplitude. A major shortcoming of these methods is that these procedures require substantial computer time where many partial waves are involved.<sup>21</sup> In order to avoid this difficulty we propose a new procedure for evaluating the Glauber amplitude. This procedure leads to a two-dimensional integral for the amplitude, which can be computed numerically with convenience and without the sort of difficulty seemingly inherent in the partial-wave techniques.

The plan of this paper is as follows. Section II gives the theoretical formulation of obtaining the

TDCS for electron-impact ionization of hydrogen in the GA. In that section we describe the reduction of the  $H(e, 2e)H^*$  amplitude to a two-dimensional integral. In Sec. III, we present the results of our numerical calculation of the TDCS. Moreover, we have recalculated via our new procedure the doubly-differential cross sections (DDCS) (differential in scattering angle and energy of the ejected electron). Our results for the DDCS are in agreement with those previously obtained by Tsuji *et al.* using the partial-wave technique. Thus we demonstrate that the present procedure is valid and useful for performing actual calculations. In this section, we compare our TDCS results with those of the FBA and experiment. Section IV contains the conclusions. Atomic units (a.u.) are used throughout.

## II. THEORY

The Glauber amplitude for the ionization of atomic hydrogen by electron impact is given by<sup>13</sup>

$$F(\vec{q}, \vec{k}_2) = \frac{ik}{2\pi} \int d\vec{b} d\vec{r} X_c^*(\vec{k}_2, \vec{r}) \left[ 1 - \left( \frac{|\vec{b} - \vec{s}|}{b} \right)^{2i\eta} \right] \times u_0(\vec{r}) e^{i\vec{q} \cdot \vec{b}}, \quad (1)$$

where  $\vec{q} = \vec{k} - \vec{k}_1$  and  $\eta = 1/k$ . Here  $\vec{k}$ ,  $\vec{k}_1$ , and  $\vec{k}_2$  are the momenta of the incoming, scattered, and ejected electrons, respectively, and  $\vec{q}$  represents the momentum transfer.  $\vec{b}$  and  $\vec{s}$  are the respective projections of the position vectors of the incident particle and the bound electron onto the plane perpendicular to the direction of the Glauber path integration.<sup>22</sup> In Eq. (1),  $\vec{q}$ ,  $\vec{b}$ , and  $\vec{s}$  are coplanar,  $u_0(\vec{r})$  represents the wave function of the initial state of the target and is given by

$$u_0(\vec{r}) = \lambda^{3/2} \pi^{-1/2} e^{-\lambda r}, \quad (2)$$

while  $X_c^*(\vec{k}_2, \vec{r})$  denotes the wave function of the ejected electron and is taken to be the Coulomb wave function

$$X_c^*(\vec{k}_2, \vec{r}) = (2\pi)^{-3/2} e^{i\gamma r/2} \Gamma(1 - i\gamma) e^{-i\vec{k}_2 \cdot \vec{r}} \times {}_1F_1(i\gamma, 1, i(k_2 r + \vec{k}_2 \cdot \vec{r})), \quad (3)$$

with  $\lambda = 1$  and  $\gamma = 1/k_2$ .

Using Eqs. (2) and (3) in Eq. (1) we can express the scattering amplitude as

$$F(\vec{q}, \vec{k}_2) = C \frac{\partial}{\partial \lambda} I(\vec{q}, \vec{k}_2), \quad (4)$$

where the generating function  $I$  is defined by

$$I(\vec{q}, \vec{k}_2) = \int d\vec{b} d\vec{r} \frac{e^{-\lambda r}}{r} e^{-i\vec{k}_2 \cdot \vec{r} + i\vec{q} \cdot \vec{b}} \times {}_1F_1(i\gamma, 1, i(k_2 r + \vec{k}_2 \cdot \vec{r})) \left( \frac{|\vec{b} - \vec{s}|}{b} \right)^{2i\eta} \quad (5)$$

and

$$C = 2^{-5/2} i k \pi^{-3} e^{i\gamma r/2} \Gamma(1 - i\gamma). \quad (6)$$

Equation (4) is obtained by dropping the first term within the square bracket under the integral in Eq. (1), since this term leads to a  $\delta$  function in  $\vec{q}$  and contributes nothing to the integral in the present case where  $q$  is always nonzero.

In order to facilitate the evaluation of the scattering amplitude, we consider, instead of  $I$ , the integral

$$J(\vec{q}, \vec{k}_2, \epsilon_1, \epsilon_2) = \int d\vec{b} d\vec{r} \frac{e^{-\lambda r}}{r} e^{-i\vec{k}_2 \cdot \vec{r} + i\vec{q} \cdot \vec{b}} \times {}_1F_1(i\gamma, 1, i(k_2 r + \vec{k}_2 \cdot \vec{r})) \times |\vec{b} - \vec{s}|^{2i\eta} b^{-2i\eta} \epsilon_2. \quad (7)$$

In the course of the evaluation of the amplitude we changed the order of integrations, wherever necessary, and the infinitesimally small positive quantities  $\epsilon_1$  and  $\epsilon_2$  introduced here guarantee the convergence requirements at all stages.

We next introduce the following integral representation of the confluent hypergeometric function<sup>23</sup>:

$${}_1F_1(ix, 1, \omega) = \frac{1}{2\pi i} \oint_{\Gamma} dt t^{-1+ix} (t-1)^{-ix} e^{\omega t}, \quad (8)$$

where  $\Gamma$  indicates a closed contour encircling each of the two points 0 and 1 once counterclockwise. On using Eq. (8) in Eq. (7) we have

$$J(\vec{q}, \vec{k}_2, \epsilon_1, \epsilon_2) = \frac{1}{2\pi i} \oint_{\Gamma} dt t^{-1+i\gamma} (t-1)^{-i\gamma} \times \int d\vec{b} d\vec{r} \frac{e^{-\Lambda r}}{r} e^{i\vec{k}_2 \cdot \vec{r} + i\vec{q} \cdot \vec{b}} \times b^{-2i\eta} \epsilon_2 (|\vec{b} - \vec{s}|)^{2i\eta} \epsilon_1, \quad (9)$$

with  $\Lambda = \lambda - ik_2 t$  and  $\vec{K}_2 = \vec{k}_2(t-1)$ . We then replace  $e^{-\Lambda r}/r$  by its Fourier transform

$$\frac{e^{-\Lambda r}}{r} = \frac{1}{2\pi^2} \int d\vec{p} \frac{e^{i\vec{p} \cdot \vec{r}}}{p^2 + \Lambda^2},$$

and introduce cylindrical coordinates for  $\vec{p}$  and  $\vec{r}$ :  $\vec{p} = \vec{p}_\rho + \vec{p}_z$  and  $\vec{r} = \vec{s} + \vec{z}$ . Moreover, to express the  $J$  integral in a form separable in the integration variables, we introduce the transformation  $\vec{s} - \vec{b} = \vec{s}'$ . Consequently, Eq. (9) becomes

$$J(\vec{q}, \vec{k}_2, \epsilon_1, \epsilon_2) = \frac{1}{4\pi^3 i} \oint_{\Gamma} dt t^{-1+i\gamma} (t-1)^{-i\gamma} \int d^2 b d^2 s' dz d^2 p_\rho dp_z \times \frac{\exp[i(\vec{p}_\rho + \vec{K}_{2\rho}) \cdot \vec{s}' + i(p_z + K_{2z})z + i(\vec{p}_\rho + \vec{K}_{2\rho}) \cdot \vec{b} + i\vec{q} \cdot \vec{b}]}{p_\rho^2 + p_z^2 + \Lambda^2} s'^{2i\eta} b^{-2i\eta} \epsilon_2. \quad (10)$$

On carrying out the  $z$  integration we get a  $\delta$  function in  $(p_x + K_{2x})$ . The evaluation of the  $p$  integral can now be easily performed, and we have

$$J(\vec{q}, \vec{k}_2, \epsilon_1, \epsilon_2) = \frac{1}{2\pi^2 i} \oint_{\Gamma} dt t^{-1+i\gamma} (t-1)^{-i\gamma} \int d^2b d^2s d^2p_\rho \frac{\exp[i(\vec{p}_\rho + \vec{K}_{2\rho}) \cdot \vec{s} + i(\vec{p}_\rho + \vec{K}_{2\rho}) \cdot \vec{b} + i\vec{q} \cdot \vec{b}]}{p_\rho^2 + K_{2z}^2 + \Lambda^2} s^{2i\eta - \epsilon_1} b^{-2i\eta - \epsilon_2}. \quad (11)$$

The azimuthal angle integrations for the vectors  $\vec{b}$  and  $\vec{s}$  can be done using the relation<sup>24</sup>

$$\int_0^{2\pi} d\phi e^{iqb \cos\phi + im\phi} = 2\pi i^m J_m(qb)$$

and we get

$$J(\vec{q}, \vec{k}_2, \epsilon_1, \epsilon_2) = \frac{2}{i} \oint_{\Gamma} dt t^{-1+i\gamma} (t-1)^{-i\gamma} \int d^2p_\rho \frac{1}{p_\rho^2 + K_{2z}^2 + \Lambda^2} \int_0^\infty db b^{-2i\eta+1-\epsilon_2} J_0(|\vec{p}_\rho + \vec{K}_{2\rho} + \vec{q}|b) \times \int_0^\infty ds s^{2i\eta+1-\epsilon_1} J_0(|\vec{p}_\rho + \vec{K}_{2\rho}|s). \quad (12)$$

We note that<sup>25</sup>

$$\int_0^\infty e^{-\alpha x} J_\nu(\beta x) x^{\mu-1} dx = \frac{(\frac{1}{2}\beta)^\nu \Gamma(\nu + \mu)}{[(\alpha^2 + \beta^2)^{\nu+\mu}]^{1/2} \Gamma(\nu+1)} {}_2F_1\left(\frac{\nu + \mu}{2}, \frac{1 - \mu + \nu}{2}; \nu + 1; \frac{\beta^2}{\alpha^2 + \beta^2}\right) \quad [\text{Re}(\nu + \mu) > 0, \text{Re}(\alpha + i\beta) > 0, \text{Re}(\alpha - i\beta) > 0].$$

Then taking the limit  $\alpha \rightarrow 0+$  in the above result and utilizing the identity<sup>26</sup>

$${}_2F_1(a, b; c; 1) = \frac{\Gamma(c)\Gamma(c-a-b)}{\Gamma(c-a)\Gamma(c-b)} \quad [c \neq 0, -1, -2, \dots, \text{Re}(c-a-b) > 0],$$

we have

$$J(\vec{q}, \vec{k}_2, \epsilon_1, \epsilon_2) = \frac{2D_1 D_2}{i} \oint_{\Gamma} dt t^{-1+i\gamma} (t-1)^{-i\gamma} \times \int d^2p_\rho \frac{1}{(p_\rho^2 + K_{2z}^2 + \Lambda^2) |\vec{p}_\rho + \vec{K}_{2\rho}|^{2+2i\eta-\epsilon_1} |\vec{p}_\rho + \vec{K}_{2\rho} + \vec{q}|^{2-2i\eta-\epsilon_2}}, \quad (13)$$

where

$$D_1 = \frac{\Gamma(\frac{1}{2})\Gamma(2-2i\eta-\epsilon_2)}{\Gamma(i\eta+\epsilon_2/2)\Gamma(\frac{3}{2}-i\eta-\epsilon_2/2)}$$

and

$$D_2 = \frac{\Gamma(\frac{1}{2})\Gamma(2+2i\eta-\epsilon_1)}{\Gamma(-i\eta+\epsilon_1/2)\Gamma(\frac{3}{2}+i\eta-\epsilon_1/2)}.$$

On replacing  $\vec{p}_\rho + \vec{K}_{2\rho} + \vec{q}$  by  $\vec{p}_\rho$ , Eq. (13) can be written as

$$J(\vec{q}, \vec{k}_2, \epsilon_1, \epsilon_2) = \frac{2D_1 D_2}{i} \int d^2p_\rho \frac{1}{p_\rho^{2-2i\eta-\epsilon_2} |\vec{p}_\rho - \vec{q}|^{2+2i\eta-\epsilon_1}} T, \quad (14)$$

where

$$T = \oint_{\Gamma} dt t^{-1+i\gamma} (t-1)^{-i\gamma} \frac{1}{k_{2z}^2(t-1)^2 + (\lambda - ik_2 t)^2 + [|\vec{p}_\rho - \vec{q} - \vec{K}_{2\rho}(t-1)|]^2}. \quad (15)$$

In order to evaluate the  $T$  integral, we express Eq. (15) in the following form:

$$T = \oint_{\Gamma} dt t^{-1+i\gamma} (t-1)^{-i\gamma} V(t), \quad (16)$$

where

$$V(t) = 1/(A - Bt) \quad (17)$$

with

$$A = k_2^2 + \lambda^2 + (\vec{p}_\rho - \vec{q})^2 + 2(\vec{p}_\rho - \vec{q}) \cdot \vec{K}_{2\rho}, \quad (18)$$

$$B = 2[k_2^2 + i\lambda k_2 + (\vec{p}_\rho - \vec{q}) \cdot \vec{K}_{2\rho}]. \quad (19)$$

The quantity  $V(t)$  has one singularity, a simple pole, at  $t = \tau = A/B$ .  $\tau$  lies outside the  $t$  contour. The  $t$  integrand in Eq. (16) is single valued and

$O(1/t^2)$  as  $t \rightarrow \infty$ , so that the integral over a circular contour of infinite radius vanishes. This, however, by Cauchy's theorem is the sum of our required integral and  $2\pi i$  times the residue at  $\tau$ . Thus

$$T = 2\pi i (\tau - 1)^{-i\gamma} \tau^{i\gamma} / A. \quad (20)$$

The scattering amplitude which is related to the derivative of  $J$  with respect to  $\lambda$  in the limit  $\epsilon_1 \rightarrow 0+$  and  $\epsilon_2 \rightarrow 0+$  can now be written as

$$F(\vec{q}, \vec{k}_2) = \lim_{\epsilon_1 \rightarrow 0+, \epsilon_2 \rightarrow 0+} 4\pi C D_1 D_2 K, \quad (21)$$

where

$$K = \int d^2 p_\rho \frac{C_1 A^{i\gamma-2} (A-B)^{-i\gamma} + C_2 A^{i\gamma-1} (A-B)^{-i\gamma-1}}{p_\rho^{2-2i\gamma-\epsilon_2} |\vec{p}_\rho - \vec{q}|^{2+2i\gamma-\epsilon_1}} \quad (22)$$

with  $C_1 = 2\lambda(i\gamma - 1)$  and  $C_2 = -2i\gamma(\lambda - ik)$ .

We see that the integrand of the  $K$  integral has strong singularities at  $p_\rho = 0$  and  $\vec{p}_\rho = \vec{q}$  and that the integral cannot be evaluated when  $\epsilon_1$  and  $\epsilon_2$  are made zero. In order to avoid this difficulty, we evaluate the integral after subtracting a term which can be integrated analytically. The singularity of the remaining integrand is now sufficiently mild so

that the numerical evaluation is possible when  $\epsilon_1$  and  $\epsilon_2$  are zero.

We can now write

$$K = \int d^2 p_\rho \frac{f(\vec{p}_\rho) - \left( \frac{|\vec{p}_\rho - \vec{q}|}{q} f(p_\rho = 0) + \frac{p_\rho}{q} f(\vec{p}_\rho = \vec{q}) \right)}{p_\rho^{2-2i\gamma-\epsilon_2} |\vec{p}_\rho - \vec{q}|^{2+2i\gamma-\epsilon_1}} + S, \quad (23)$$

where

$$f(\vec{p}_\rho) = C_1 A^{i\gamma-2} (A-B)^{-i\gamma} + C_2 A^{i\gamma-1} (A-B)^{-i\gamma-1} \quad (24)$$

and

$$S = \int d^2 p_\rho \frac{\frac{|\vec{p}_\rho - \vec{q}|}{q} f(p_\rho = 0) + \frac{p_\rho}{q} f(\vec{p}_\rho = \vec{q})}{p_\rho^{2-2i\gamma-\epsilon_2} |\vec{p}_\rho - \vec{q}|^{2+2i\gamma-\epsilon_1}}. \quad (25)$$

In order to be able to perform the  $S$  integral analytically, we introduce polar coordinates  $p$  and  $\phi$  for the vector  $\vec{p}_\rho$ ;  $\phi$  denotes the angle between  $\vec{p}_\rho$  and  $\vec{q}$ . Equation (25) can then be written as

$$S = q^{-1} [f(p_\rho = 0) S_1(\vec{q}, \eta, \epsilon_1, \epsilon_2) + f(\vec{p}_\rho = \vec{q}) S_1(-\vec{q}, -\eta, \epsilon_2, \epsilon_1)], \quad (26)$$

where

$$S_1(\vec{q}, \eta, \epsilon_1, \epsilon_2) = \int_0^\infty \int_0^{2\pi} dp d\phi \frac{1}{p^{1-2i\gamma-\epsilon_2} (p^2 + q^2 - 2pq \cos \phi)^{1/2+2i\gamma-\epsilon_1/2}}. \quad (27)$$

Now we take advantage of the relation<sup>27</sup>

$$\frac{1}{2\pi} \int_0^{2\pi} \frac{\cos(n\phi) d\phi}{(1 - 2z \cos \phi + z^2)^\alpha} = \frac{\Gamma(\alpha + n)}{\Gamma(\alpha) n!} z^n {}_2F_1(\alpha, \alpha + n; 1 + n; z^2),$$

provided

$$n = 0, 1, 2, \dots, \quad \alpha \neq 0, -1, -2, \dots, \quad |z| < 1,$$

and perform the  $\phi$  integration. We note that  $|z|$  is to be less than unity. So we have divided the range of the integration variable  $p$  into two parts, namely, 0 to  $q$  and  $q$  to  $\infty$ . Thus Eq. (27) reduces to

$$S_1(\vec{q}, \eta, \epsilon_1, \epsilon_2) = 2\pi q^{-1+\epsilon_1+\epsilon_2} \left( \int_0^1 dz z^{2i\gamma-1+\epsilon_2} {}_2F_1\left(\frac{1}{2} + i\eta - \frac{1}{2}\epsilon_1, \frac{1}{2} + i\eta - \frac{1}{2}\epsilon_1; 1; z^2\right) + \int_0^1 dz z^{-\epsilon_1+\epsilon_2} {}_2F_1\left(\frac{1}{2} + i\eta - \frac{1}{2}\epsilon_1, \frac{1}{2} + i\eta - \frac{1}{2}\epsilon_1; 1; z^2\right) \right). \quad (28)$$

Next we utilize the series representation of the Gaussian hypergeometric function and perform the integration over  $z$  term by term. We obtain

$$S_1(\vec{q}, \eta, \epsilon_1, \epsilon_2) = 2\pi q^{-1+\epsilon_1+\epsilon_2} \sum_{r=0}^{\infty} \frac{(\frac{1}{2} + i\eta - \frac{1}{2}\epsilon_1)_r (\frac{1}{2} + i\eta - \frac{1}{2}\epsilon_1)_r}{(1)_r r!} \left( \frac{1}{2(r+i\eta) + \epsilon_2} + \frac{1}{2r+1 - \epsilon_1 - \epsilon_2} \right), \quad (29)$$

where  $(a)_r$  is Pochhammer's symbol.<sup>28</sup>

Finally, we take the limit of the function  $K$  in Eq. (23) as  $\epsilon_1 \rightarrow 0+$  and  $\epsilon_2 \rightarrow 0+$ , and express the scattering amplitude as

$$F(\vec{q}, \vec{k}_2) = 2^{3/2} ik \pi^{-2} \eta^2 e^{\pi/2} \Gamma(1 - i\gamma) \left( 2\pi q^{-2} [f(p_\rho = 0) H(\eta) + f(\vec{p}_\rho = \vec{q}) H(-\eta)] + \int_0^\infty dp \frac{1}{p^{1-2i\gamma}} \int_0^{2\pi} d\phi \frac{f(\vec{p}_\rho) - q^{-1} [(p^2 + q^2 - 2pq \cos \phi)^{1/2} f(p_\rho = 0) + p_\rho f(\vec{p}_\rho = \vec{q})]}{(p^2 + q^2 - 2pq \cos \phi)^{1+i\gamma}} \right), \quad (30)$$

TABLE I. Coplanar ( $\Phi_1 = 0^\circ$ ,  $\Phi_2 = \pi$ ) triply-differential cross sections,  $d^3\sigma/d\hat{k}_1 d\hat{k}_2 dE_2$ , for electron-impact ionization of atomic hydrogen in the FBA and the GA for the incident energy of 100 eV. The format  $AB$  stands for  $A \times 10^B$ .

$E_2$ (eV)	$\theta_1$ (deg)	$\theta_2$ (deg)	FBA <sup>a</sup>	GA <sup>b</sup>	$\theta_2$ (deg)	FBA	GA	$\theta_2$ (deg)	FBA	GA
25	20	0	3.24 -2	1.96 -2	55	5.64 -1	3.83 -1	110	6.62 -3	4.75 -3
		10	8.85 -2	5.32 -2	60	4.53 -1	3.01 -1	120	4.78 -3	3.79 -3
		20	2.17 -1	1.36 -1	65	3.36 -1	2.17 -1	130	4.33 -3	3.80 -3
		30	4.31 -1	2.85 -1	70	2.34 -1	1.47 -1	140	4.18 -3	4.13 -3
		35	5.44 -1	3.69 -1	75	1.54 -1	9.42 -2	150	4.04 -3	4.58 -3
		40	6.32 -1	4.36 -1	80	9.68 -2	5.83 -2	160	3.87 -3	5.06 -3
		45	6.69 -1	4.64 -1	90	3.56 -2	2.15 -2	170	3.69 -3	5.51 -3
	50	6.43 -1	4.44 -1	100	1.35 -2	8.67 -3	180	3.53 -3	5.90 -3	
	30	0	1.47 -2	9.96 -3	55	6.53 -1	3.77 -1	110	7.80 -3	5.26 -3
		10	3.67 -2	2.35 -2	60	5.51 -1	3.17 -1	120	4.69 -3	2.90 -3
		20	1.01 -1	6.03 -2	65	4.16 -1	2.40 -1	130	3.35 -3	1.88 -3
		30	2.58 -1	1.50 -1	70	2.87 -1	1.66 -1	140	2.63 -3	1.46 -3
		35	3.81 -1	2.20 -1	75	1.85 -1	1.08 -1	150	2.18 -3	1.34 -3
		40	5.18 -1	2.98 -1	80	1.14 -1	6.80 -2	160	1.87 -3	1.38 -3
45		6.32 -1	3.65 -1	90	4.16 -2	2.64 -2	170	1.64 -3	1.50 -3	
50	6.85 -1	3.95 -1	100	1.63 -2	1.10 -2	180	1.47 -3	1.67 -3		
36.4	20	0	2.58 -2	1.52 -2	55	1.24 -1	8.50 -2	110	1.20 -3	1.08 -3
		10	7.14 -2	4.58 -2	60	8.23 -2	5.36 -2	120	1.15 -3	1.12 -3
		20	1.58 -1	1.12 -1	65	5.14 -2	3.19 -2	130	1.14 -3	1.21 -3
		30	2.48 -1	1.90 -1	70	3.05 -2	1.83 -2	140	1.11 -3	1.31 -3
		35	2.66 -1	2.07 -1	75	1.75 -2	1.02 -2	150	1.06 -3	1.42 -3
		40	2.57 -1	1.98 -1	80	9.88 -3	5.75 -3	160	1.01 -3	1.53 -3
		45	2.22 -1	1.66 -1	90	3.29 -3	2.12 -3	170	9.59 -4	1.64 -3
	50	1.73 -1	1.25 -1	100	1.55 -3	1.23 -3	180	9.17 -4	1.74 -3	
	30	0	1.01 -2	6.99 -3	55	2.45 -1	1.56 -1	100	2.48 -3	1.97 -3
		10	3.27 -2	2.07 -2	60	1.63 -1	1.02 -1	120	1.10 -3	7.91 -4
		20	1.02 -1	6.35 -2	65	9.92 -2	6.17 -2	130	8.95 -4	6.34 -4
		30	2.49 -1	1.59 -1	70	5.70 -2	3.55 -2	140	7.61 -4	5.74 -4
		35	3.32 -1	2.14 -1	75	3.17 -2	2.01 -2	150	6.61 -4	5.69 -4
		40	3.85 -1	2.50 -1	80	1.75 -2	1.15 -2	160	5.84 -4	5.98 -4
45		3.84 -1	2.49 -1	85	9.85 -3	6.80 -3	170	5.25 -4	6.50 -4	
50	3.28 -1	2.12 -1	90	5.78 -3	4.24 -3	180	4.80 -4	7.19 -4		
40	0	6.06 -3	4.09 -3	55	2.42 -1	1.40 -1	110	1.34 -3	7.90 -4	
	10	1.78 -2	1.13 -2	60	1.61 -1	9.34 -2	120	8.63 -4	4.20 -4	
	20	5.80 -2	3.46 -2	65	9.67 -2	5.68 -2	130	6.18 -4	2.53 -4	
	30	1.68 -1	9.75 -2	70	5.48 -2	3.28 -2	140	4.73 -4	1.82 -4	
	35	2.50 -1	1.44 -1	75	3.03 -2	1.87 -2	150	3.80 -4	1.60 -4	
	40	3.22 -1	1.86 -1	80	1.69 -2	1.08 -2	160	3.16 -4	1.65 -4	
	45	3.50 -1	2.02 -1	90	5.79 -3	3.91 -3	170	2.72 -4	1.89 -4	
50	3.17 -1	1.83 -1	100	2.48 -3	1.65 -3	180	2.40 -4	2.27 -4		

<sup>a</sup> Present first Born approximation.

<sup>b</sup> Present Glauber approximation.

where

$$H(\eta) = \sum_{r=0}^{\infty} \frac{(\frac{1}{2} + i\eta)_r (\frac{1}{2} + i\eta)_r}{(1)_{r!}} \left( \frac{1}{2(r+i\eta)} + \frac{1}{2r+1} \right). \quad (31)$$

The triply-differential cross section for electron-impact ionization of atomic hydrogen is given by<sup>29</sup>

$$\frac{d^3\sigma}{d\hat{k}_1 d\hat{k}_2 dE_2} = \frac{k_1 k_2}{k} |F(\vec{q}, \vec{k}_2)|^2, \quad (32)$$

where  $d\hat{k}_1$  and  $d\hat{k}_2$  denote, respectively, the ele-

ments of solid angle for the scattered and ejected electrons, and  $dE_2$  represents the energy interval of the ejected electron.

### III. NUMERICAL RESULTS AND DISCUSSION

#### A. Numerical procedure

In order to check the numerical program developed for the present calculation, we have recalculated the DDCS in the GA for electron-impact

TABLE II. Coplanar ( $\Phi_1 = 0^\circ$ ,  $\Phi_2 = \pi$ ) triply-differential cross sections,  $d^3\sigma/dk_1 d\hat{k}_2 dE_2$ , for electron-impact ionization of atomic hydrogen in the FBA and the GA for the incident energy  $E = 113.6$  eV and the ejected electron energy  $E_2 = 50$  eV. The format  $AB$  stands for  $A \times 10^B$ .

$\theta_1$ (deg)	$\theta_2$ (deg)	FBA <sup>a</sup>	GA <sup>b</sup>	$\theta_2$ (deg)	FBA	GA	$\theta_2$ (deg)	FBA	GA
35	0	4.04 -3	3.01 -3	55	9.84 -2	6.52 -2	100	6.25 -4	5.34 -4
	10	1.53 -2	1.03 -2	60	5.49 -2	3.62 -2	120	2.96 -4	2.08 -4
	20	5.76 -2	3.79 -2	65	2.87 -2	1.90 -2	130	2.34 -4	1.57 -4
	30	1.62 -1	1.08 -1	70	1.45 -2	9.81 -3	140	1.92 -4	1.33 -4
	35	2.17 -1	1.47 -1	75	7.35 -3	5.19 -3	150	1.62 -4	1.26 -4
	40	2.40 -1	1.63 -1	80	3.85 -3	2.89 -3	160	1.40 -4	1.28 -4
	45	2.14 -1	1.45 -1	85	2.14 -3	1.72 -3	170	1.24 -4	1.39 -4
	50	1.57 -1	1.05 -1	90	1.30 -3	1.09 -3	180	1.12 -4	1.58 -4
45	0	2.67 -3	1.90 -3	55	9.54 -2	5.95 -2	100	5.99 -4	3.98 -4
	10	9.15 -3	6.15 -3	60	5.25 -2	3.31 -2	120	2.24 -4	1.01 -4
	20	3.57 -2	2.27 -2	65	2.69 -2	1.73 -2	130	1.60 -4	6.02 -5
	30	1.18 -1	7.36 -2	70	1.36 -2	8.96 -3	140	1.22 -4	4.20 -5
	35	1.76 -1	1.09 -1	75	6.97 -3	4.75 -3	150	9.73 -5	3.58 -5
	40	2.13 -1	1.32 -1	80	3.74 -3	2.63 -3	160	8.06 -5	3.65 -5
	45	2.02 -1	1.26 -1	85	2.13 -3	1.53 -3	170	6.89 -5	4.23 -5
	50	1.53 -1	9.49 -2	90	1.31 -3	9.38 -4	180	6.08 -5	5.30 -5

<sup>a</sup> Present first Born approximation.

<sup>b</sup> Present Glauber approximation.

ionization of atomic hydrogen and compared our results with the corresponding available values of Tsuji *et al.*, obtained previously with the use of partial-wave technique. The two-dimensional integral in Eq. (30) was evaluated by dividing the range of the  $p$  integral into two parts: (i)  $0 \leq p \leq q$  and (ii)  $q \leq p \leq \infty$ . Then, in the region (i) we used the transformation  $p = qe^{-x}$ , whereas in (ii) we adopted  $p^2 = q^2(2e^y - 1)$ , and performed the integration via Gauss-Laguerre quadrature. The  $\phi$  integral was performed using Gauss-Legendre quadrature. We have found that the DDCS calculated using the present method are in excellent agreement with those of Tsuji *et al.*

We now turn to the calculation of TDCS. A noteworthy point is that whereas the magnitudes of DDCS are not dependent upon the choice of the direction of  $z$  axis, the TDCS values are relevant to the choice of  $\hat{z}$  direction. In the formalism developed in Sec. II, we have not specified in particular our choice of the direction of  $z$  axis. McGuire *et al.*<sup>13</sup> have pointed out that the direction of  $z$  axis must be taken perpendicular to the direction of momentum transfer in order to give agreement with the results of Born approximation. Earlier it was stressed by Gerjuoy<sup>30</sup> that the Born approximation may be recovered from the GA by keeping the first nonzero term of an expansion of  $(1 - e^{\chi})$  in powers of  $\chi$  only if  $\hat{z}$  is perpendicular to  $\vec{q}$ . If a different choice is made, such as,  $\hat{z}$  is parallel to the incident beam direction  $\vec{k}$ , the angular distributions for the ejected electrons differ substan-

tially, according to McGuire *et al.*, from the predictions of the FBA at incident energies as large as 500 eV or more. We have also noticed similar features. For example, at an incident energy of 100 eV and ejected energy of 0.1 eV with  $\theta_1 = \theta_2 = \Phi_2 = 0$ , the TDCS obtained in the GA with the  $z$  axis (i) parallel to  $\vec{k}$ , and (ii) along a direction perpendicular to  $\vec{q}$  are, respectively, 1.92 and 416 against the corresponding FBA value of 427. Since the GA results are expected to be in close agreement with the FBA findings at high incident energies with slow ejected electrons we have performed the TDCS calculations only with the second choice.

For the evaluation of TDCS, the important quantity  $Q$  that needs be considered is  $(\vec{p}_p - \vec{q}) \cdot \vec{k}_{2p}$  occurring in the expression for  $f(\vec{p}_p)$  in Eq. (30). We follow the notation of Ehrhardt *et al.*<sup>31</sup> in designating the two emerging electrons as 1 and 2, where 1 represents the electron whose direction is held fixed while the direction of electron 2 is varied. We choose the  $x$  direction to correspond to  $\theta_1 = \pi/2$ ,  $\Phi_1 = 0$ . The direction of electron 2 is now given by the angles  $\theta_2$  and  $\Phi_2$ . In the following we shall consider only the case of coplanar incident and emerging electron beams, i.e.,  $\Phi_2 = 0$  or  $\pi$ .

#### Choice 1: $\hat{z}$ is parallel to $\vec{k}$

We choose  $\vec{q}$  along the  $x$  direction in the  $x$ - $y$  plane. In the GA, since  $q_z$  is zero the expression for  $Q$  is given by

$$Q = pk_2 \sin\theta_2 \cos(\phi - \Phi_2) - qk_2 \sin\theta_2 \cos\Phi_2. \quad (33)$$

TABLE III. Coplanar ( $\Phi_1=0^\circ$ ,  $\Phi_2=\pi$ ) triply-differential cross sections,  $d^3\sigma/d\hat{k}_1 d\hat{k}_2 dE_2$ , for electron-impact ionization of atomic hydrogen in the FBA and the GA for the incident energy  $E=250$  eV and the ejected electron energy  $E_2=50$  eV. The format  $AB$  stands for  $A \times 10^B$ .

$\theta_1$ (deg)	$\theta_2$ (deg)	FBA <sup>a</sup>	GA <sup>b</sup>	$\theta_2$ (deg)	FBA	GA	$\theta_2$ (deg)	FBA	GA
15	0	1.22 -3	8.00 -4	55	1.24 -1	1.12 -1	100	2.82 -3	1.82 -3
	10	4.22 -3	2.77 -3	60	1.13 -1	1.00 -1	120	4.51 -4	4.09 -4
	20	1.41 -2	1.00 -2	65	9.20 -2	7.93 -2	130	4.20 -4	4.49 -4
	30	3.93 -2	3.05 -2	70	6.80 -2	5.62 -2	140	4.47 -4	5.10 -4
	35	5.96 -2	4.85 -2	75	4.61 -2	3.64 -2	150	4.60 -4	5.54 -4
	40	8.34 -2	7.08 -2	80	2.90 -2	2.19 -2	160	4.56 -4	5.82 -4
	45	1.06 -1	9.35 -2	85	1.72 -2	1.24 -2	170	4.41 -4	6.00 -4
	50	1.21 -1	1.09 -1	90	9.73 -3	6.73 -3	180	4.22 -4	6.12 -4
20	0	8.94 -4	8.29 -4	55	2.30 -1	1.89 -1	100	3.97 -3	3.14 -3
	10	2.22 -3	1.84 -3	60	2.29 -1	1.89 -1	120	6.70 -4	6.43 -4
	20	7.69 -3	5.90 -3	65	1.93 -1	1.58 -1	130	4.88 -4	4.76 -4
	30	2.84 -2	2.17 -2	70	1.40 -1	1.12 -1	140	4.09 -4	4.03 -4
	35	5.23 -2	4.04 -2	75	8.89 -2	6.99 -2	150	3.56 -4	3.61 -4
	40	9.00 -2	7.08 -2	80	5.15 -2	3.98 -2	160	3.14 -4	3.37 -4
	45	1.41 -1	1.13 -1	85	2.80 -2	2.13 -2	170	2.78 -4	3.23 -4
	50	1.94 -1	1.59 -1	90	1.46 -2	1.11 -2	180	2.50 -4	3.18 -4
25	0	8.54 -4	7.64 -4	55	3.02 -1	2.34 -1	100	4.46 -3	3.81 -3
	10	1.82 -3	1.63 -3	60	3.27 -1	2.53 -1	120	7.79 -4	6.92 -4
	20	5.40 -3	4.56 -3	65	2.82 -1	2.18 -1	130	4.88 -4	4.08 -4
	30	2.03 -2	1.61 -2	70	1.98 -1	1.53 -1	140	3.49 -4	2.76 -4
	35	4.06 -2	3.16 -2	75	1.19 -1	9.17 -2	150	2.68 -4	2.08 -4
	40	7.86 -2	6.07 -2	80	6.42 -2	4.96 -2	160	2.15 -4	1.72 -4
	45	1.42 -1	1.09 -1	85	3.27 -2	2.56 -2	170	1.79 -4	1.54 -4
	50	2.26 -1	1.74 -1	90	1.64 -2	1.31 -2	180	1.53 -4	1.47 -4
30	0	6.48 -4	4.77 -4	60	2.35 -1	1.76 -1	130	3.60 -4	2.33 -4
	10	1.38 -3	1.09 -3	70	1.44 -1	1.08 -1	140	2.36 -4	1.35 -4
	20	3.75 -3	3.02 -3	80	4.58 -2	3.49 -2	150	1.68 -4	8.80 -5
	30	1.30 -2	1.02 -2	90	1.20 -2	9.42 -3	160	1.27 -4	6.51 -5
	40	4.95 -2	3.76 -2	100	3.51 -3	2.83 -3	170	1.01 -4	5.48 -5
	50	1.51 -1	1.14 -1	120	6.24 -4	4.57 -4	180	8.36 -5	5.18 -5
35	0	3.75 -4	2.15 -4	55	7.89 -2	5.86 -2	100	1.85 -3	1.30 -3
	10	8.02 -4	5.27 -4	60	8.57 -2	6.38 -2	120	3.48 -4	1.95 -4
	20	2.09 -3	1.48 -3	65	7.50 -2	5.57 -2	130	1.95 -4	9.00 -5
	30	6.53 -3	4.75 -3	70	5.40 -2	4.00 -2	140	1.23 -4	4.55 -5
	35	1.20 -2	8.79 -3	75	3.36 -2	2.48 -2	150	8.42 -5	2.57 -5
	40	2.19 -2	1.61 -2	80	1.91 -2	1.40 -2	160	6.19 -5	1.70 -5
	45	3.79 -2	2.80 -2	85	1.04 -2	7.62 -3	170	4.80 -5	1.38 -5
	50	5.92 -2	4.39 -2	90	5.68 -3	4.13 -3	180	3.90 -5	1.36 -5

<sup>a</sup> Present first Born approximation.

<sup>b</sup> Present Glauber approximation.

Choice 2:  $\hat{z}$  is perpendicular to  $\hat{q}$

In this choice, the  $z$  axis is taken along the Glauber path integration, which is perpendicular to  $\hat{q}$ . This means that the previous coordinate system will now be rotated about the  $y$  axis. In the new system  $x'yz'$ ,  $\hat{q}$  is along  $x'$ . So  $Q$  becomes

$$Q = \frac{pQ_1 \cos(\phi - \Phi_2)}{q \cos\Phi_2} - Q_1, \quad (34)$$

where

$$Q_1 = -k_1 k_2 \sin\theta_1 \sin\theta_2 \cos\Phi_2 + (k - k_1 \cos\theta_1) k_2 \cos\theta_2. \quad (35)$$

A prescription has been proposed by McGuire *et al.*<sup>13</sup> Their choice  $\vec{z} = \vec{k} + \alpha \vec{k}_1$  together with  $\alpha = (\vec{k} \cdot \vec{k}_1 - k^2) / (\vec{k} \cdot \vec{k}_1 - k_1^2)$  predicts identical results to ours except at  $\theta_1 = 0$ . At zero scattering angle, their prescription is not tenable since  $\vec{z}$  becomes a null vector. For convenience we have, however, calculated the DDCS using choice 1, since the DDCS are independent of the choice of  $z$  axis.

TABLE IV. Magnitudes of binary maxima for electron-impact ionization of atomic hydrogen.

$E$ (eV)	$E_2$ (eV)	$\theta_1$ (deg)	FBA <sup>a</sup>	GA <sup>b</sup>
100	25	20	0.669	0.464
		30	0.685	0.396
	36.4	20	0.267	0.207
		30	0.392	0.255
113.6	50	40	0.350	0.202
		35	0.240	0.163
		45	0.215	0.134
250	50	15	0.125	0.113
		20	0.234	0.193
		25	0.327	0.253
		30	0.235	0.176
		35	0.0858	0.0638

<sup>a</sup> Present first Born approximation.

<sup>b</sup> Present Glauber approximation.

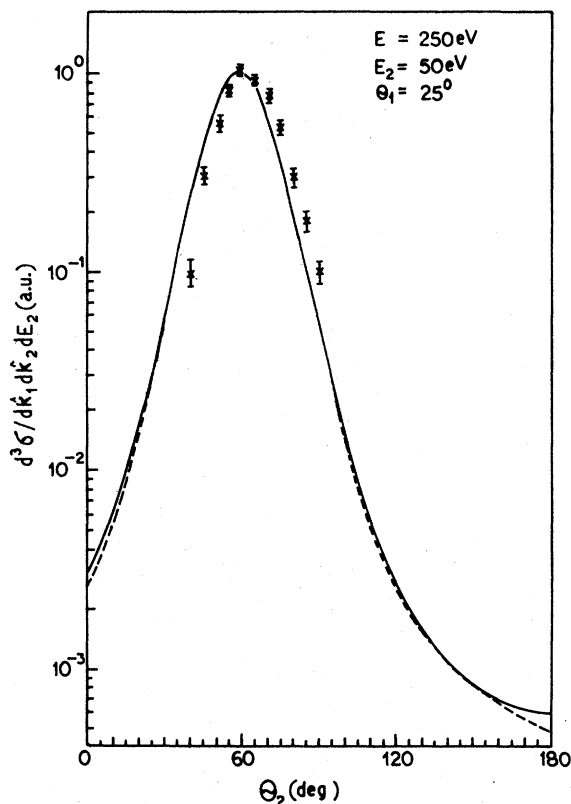


FIG. 1. Triply-differential cross sections,  $d^3\sigma/dk_1 dk_2 dE_2$  versus the angle of ejection,  $\theta_2$ , for electron-impact ionization of atomic hydrogen at the incident energy  $E=250$  eV, the energy of scattered electron  $E_1=186.4$  eV, the energy of ejected electron  $E_2=50$  eV, and the angle of scattering  $\theta_1=25^\circ$ . The solid curve is the present Glauber result ( $\times 3.94$ ). The dashed curve represents the first Born approximation results ( $\times 3.05$ ). The crosses are the experimental results of Ref. 5. All the cross sections shown are for the scattering plane  $\phi_1=0$  and  $\phi_2=\pi$ .

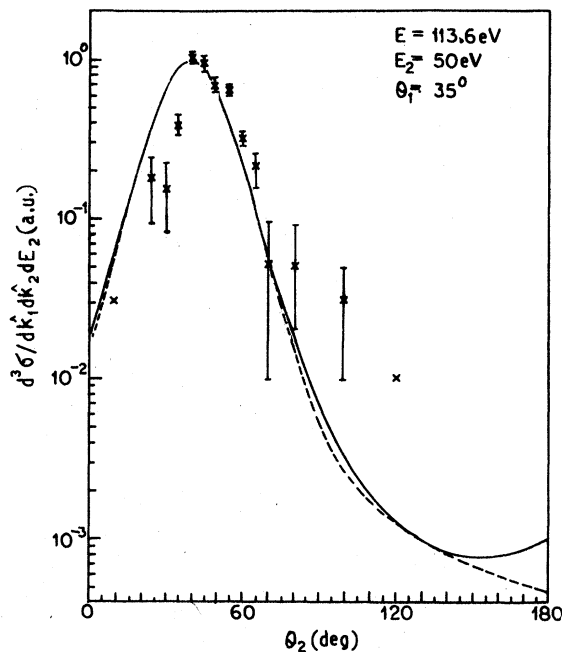


FIG. 2. Triply-differential cross sections,  $d^3\sigma/dk_1 dk_2 dE_2$  versus the angle of ejection,  $\theta_2$ , for electron-impact ionization of atomic hydrogen at the incident energy  $E=113.6$  eV, the energy of scattered electron  $E_1=50$  eV, the energy of ejected electron  $E_2=50$  eV, and the angle of scattering  $\theta_1=35^\circ$ . The solid curve is the present Glauber result ( $\times 6.15$ ). The dashed curve represents the first Born approximation results ( $\times 4.17$ ). The crosses are the experimental results of Ref. 5. All the cross sections are for the scattering plane  $\phi_1=0$  and  $\phi_2=\pi$ .

#### B. Comparison of cross sections

Tables I, II, and III present our results for the coplanar TDCS in the GA along with the corresponding FBA predictions for the ionization of atomic hydrogen by electron impact at incident energies of 100, 113.6, and 250 eV, respectively. All the reported cross sections are for the scattering plane  $\phi_2=\pi$  and obtained with the choice of  $z$  axis along the Glauber path integration, which is taken to be perpendicular to  $\vec{q}$ . The FBA cross sections are evaluated from the analytical expression given by Massey and Mohr.<sup>32</sup> An examination of the present results shows that the magnitudes of TDCS are large in the angular region  $30^\circ \leq \theta_2 \leq 90^\circ$  and that the FBA cross sections are larger than the GA values in that region. However, the results of the GA are greater than those of the FBA in the angular region where  $\theta_2$  is quite large, especially at low momentum transfers.

Both the FBA and the GA results have axial symmetry, since the scattering amplitudes in both methods are scalar functions of the vectors  $\vec{q}$  and



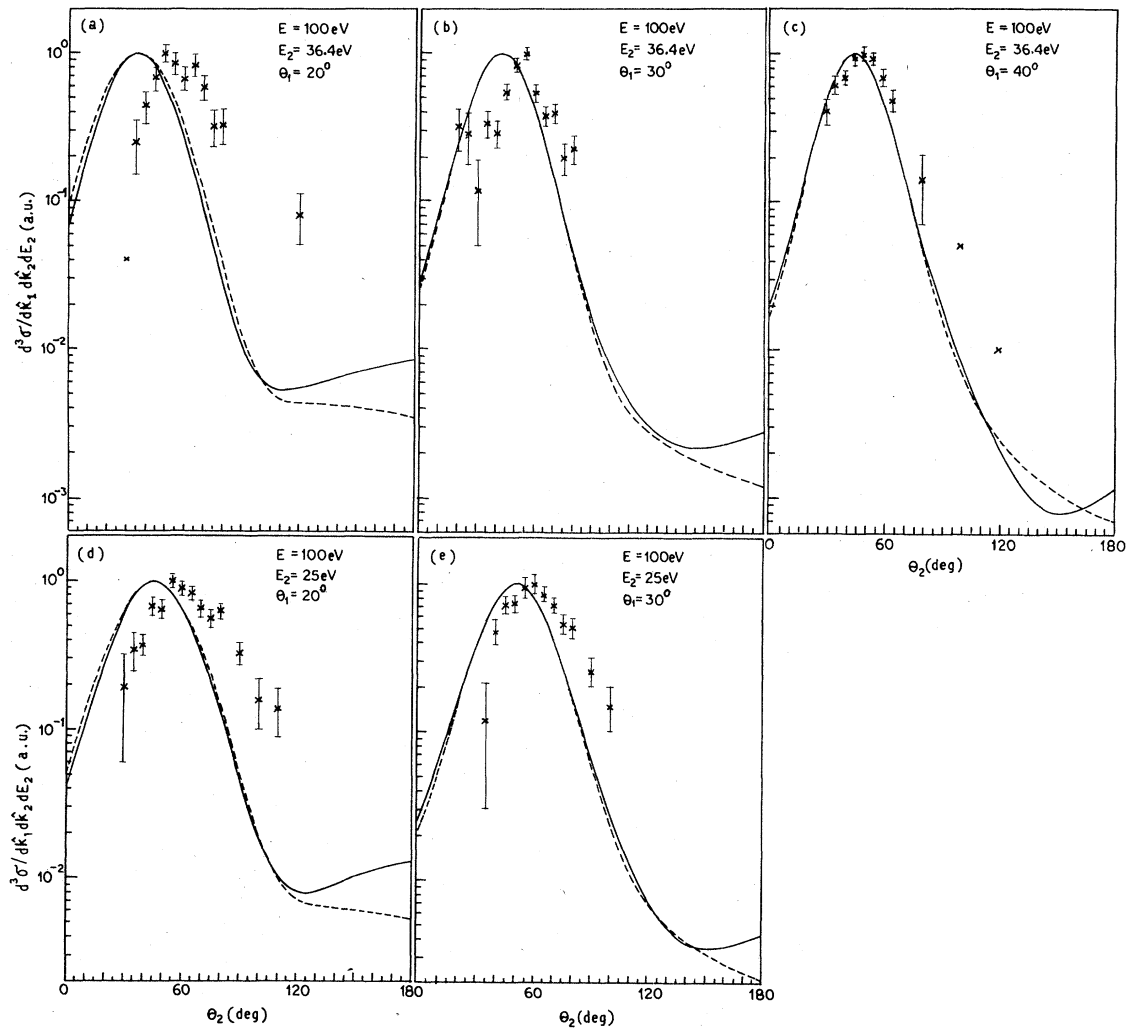


FIG. 3. Triply-differential cross sections,  $d^3\sigma/d\hat{k}_1 d\hat{k}_2 dE_2$  versus the angle of ejection,  $\theta_2$ , for electron-impact ionization of atomic hydrogen at the incident energy of 100 eV for a variety of scattered-electron energies  $E_1$ , ejected-electron energies  $E_2$ , and scattering angles  $\theta_1$ . The solid and the dashed curves represent, respectively, the present Glauber results ( $\times N_G$ ) and the first Born approximation results ( $\times N_B$ ), where  $N_G$  and  $N_B$  are the appropriate multiplication factors. (a)  $E_1=50$  eV,  $E_2=36.4$  eV,  $\theta_1=20^\circ$ ,  $N_G=4.83$ ,  $N_B=3.75$ , (b)  $E_1=50$  eV,  $E_2=36.4$  eV,  $\theta_1=30^\circ$ ,  $N_G=3.92$ ,  $N_B=2.55$ , (c)  $E_1=50$  eV,  $E_2=36.4$  eV,  $\theta_1=40^\circ$ ,  $N_G=4.96$ ,  $N_B=2.86$ , (d)  $E_1=61.4$  eV,  $E_2=25$  eV,  $\theta_1=20^\circ$ ,  $N_G=2.16$ ,  $N_B=1.50$ , and (e)  $E_1=61.4$  eV,  $E_2=25$  eV,  $\theta_1=30^\circ$ ,  $N_G=2.53$ ,  $N_B=1.46$ . The crosses are the experimental results of Ref. 5. All the cross sections shown are for the scattering plane  $\Phi_1=0$  and  $\Phi_2=\pi$ .

$\vec{k}_2$ . The magnitudes of binary peaks<sup>33</sup> obtained in the FBA and the GA are summarized in Table IV. Although the FBA- and the GA-predicted binary peak positions are the same and given by the direction of  $\vec{q}$ , the magnitudes of binary peaks obtained in these methods differ. The FBA peak values are seen to be above the corresponding magnitudes of GA peaks in all the cases considered in this work.

Figure 1 shows a comparison of the present GA calculation with the coplanar measurements of Weigold *et al.*<sup>5</sup> and with the FBA calculation for

$E=250$  eV,  $E_1=186.4$  eV, and  $E_2=50$  eV for the scattering angle of  $25^\circ$ . Since the measurements of Weigold *et al.* are relative, we have normalized the GA and the FBA cross sections to give the experimental peak height. To obtain the absolute values for cross sections the graphical results must be divided by the numbers given in brackets in the figure caption. It should be noted that the errors in the experimental data given in all the figures are the statistical errors. In fact, we have considered for comparison only those cases where the reported normalization error<sup>5</sup> is zero. We

see from Fig. 1 that the angular distribution for the ejected electron predicted by the GA is in fairly good agreement with experiment. The GA and the FBA curves are nearly indistinguishable except in the backward direction (large  $\theta_2$ ).

Figures 2 and 3 provide similar comparisons for incident energies of 113.6 and 100 eV, respectively. The agreement with experiment is seen to decrease at lower energies. One of the reasons may be that the effect of exchange is expected to be more pronounced now. Unfortunately, it is difficult to rigorously include exchange effect in the GA, because the inclusion of exchange leads to the conflict with the additivity principle in this approximation.<sup>20</sup> At the incident energy of 100 eV the angular distributions have been studied for two different energies, namely, 36.4 and 25 eV of the secondary electrons. For the ejection energy of 36.4 eV, the scattering angles considered are 20°, 30°, and 40°, while for the 25-eV ejection energy, the angles considered are 20° and 30°. We see that the agreement of the GA with experiment improves as the scattering angle begins to increase. Moreover, we find that this agreement is better as the energy of the ejected electron decreases.

#### IV. CONCLUSIONS

We have presented a method of obtaining triply-differential cross sections for electron-impact

ionization of atomic hydrogen in the Glauber approximation. This method reduces the scattering amplitude to a simple two-dimensional integral, which can be computed numerically with convenience and without the sort of difficulty seemingly inherent in the conventional partial-wave technique.

We have calculated coplanar TDCS for electron-impact ionization of atomic hydrogen at incident energies of 100, 113.6, and 250 eV for a variety of ejected electron energies and scattering angles. The present results at the incident energy of 100 eV show that the agreement of the GA with experiment improves with the increase in scattering angles. In addition, we find at this energy that for a specified scattering angle the GA gives a better fit to the experimentally observed angular distribution as the energy of the ejected electron decreases. At higher incident energies, the agreement is better. At an incident energy of 250 eV there is a fairly good agreement between the GA and experiment.

The present results show that the angular distributions of the ejected electron obtained in the GA are more or less identical with those in the FBA, except for the extreme angles. In particular, marked difference between the GA and the FBA exists in the backward direction. Since various theoretical approaches yield cross sections of different magnitudes, absolute measurements would be extremely valuable.

- <sup>1</sup>K. L. Bell and A. E. Kingston, *Advances in Atomic and Molecular Physics* (Academic, New York, 1974), Vol. 10, pp. 53-130; M. R. C. McDowell, *Atomic Processes and Applications*, edited by P. G. Burke and B. L. Moiseiwitsch (North-Holland, Amsterdam, 1976), p. 342; J. Callaway and D. H. Oza, *Phys. Lett.* **72A**, 207 (1979).
- <sup>2</sup>H. Ehrhardt, M. Schulz, T. Tekaas, and K. Willmann, *Phys. Rev. Lett.* **22**, 89 (1969).
- <sup>3</sup>H. Ehrhardt, K. H. Hesselbacher, K. Jung, and K. Willmann, *J. Phys. B* **5**, 1559 (1972); H. Ehrhardt, K. H. Hesselbacher, K. Jung, E. Schubert, and K. Willmann, *ibid.* **7**, 69 (1974); K. Jung, E. Schubert, H. Ehrhardt, and D. A. L. Paul, *ibid.* **9**, 75 (1976); S. T. Hood, I. E. McCarthy, P. J. O. Teubner, and E. Weigold, *Phys. Rev. A* **8**, 2494 (1973); R. Camilloni, G. A. Giardini, R. Tiribelli, and G. Stefani, *Phys. Rev. Lett.* **29**, 618 (1972); E. C. Beaty, K. H. Hesselbacher, S. P. Hong, and J. H. Moore, *J. Phys. B* **10**, 611 (1977); *Phys. Rev. A* **17**, 1592 (1978); G. Stefani, R. Camilloni, and A. Giardini Guidoni, *J. Phys. B* **12**, 2583 (1979); B. van Wingerden, J. T. Kimman, M. van Tilburg, E. Weigold, C. J. Joachain, B. Piraux, and F. J. de Heer, *ibid.* **12**, L627 (1979).
- <sup>4</sup>E. Weigold, S. T. Hood, I. Fuss, and A. J. Dixon, *J. Phys. B* **10**, L623 (1977).
- <sup>5</sup>E. Weigold, C. J. Noble, S. T. Hood, and I. Fuss, *J. Phys. B* **12**, 291 (1979).
- <sup>6</sup>L. D. Landau and E. M. Lifshitz, *Quantum Mechanics: Non-Relativistic Theory* (Pergamon, London, 1958), p. 458.
- <sup>7</sup>S. Geltman, *J. Phys. B* **4**, 1288 (1971); **7**, 1994 (1974); S. Geltman and M. B. Hidalgo, *ibid.* **7**, 831 (1974).
- <sup>8</sup>M. Lal, A. N. Tripathi, and M. K. Srivastava, *J. Phys. B* **12**, 945 (1979).
- <sup>9</sup>J. J. Smith, K. H. Winters, and B. H. Bransden, *J. Phys. B* **12**, 1723 (1979).
- <sup>10</sup>See, for example, E. Gerjuoy and B. K. Thomas, *Rep. Prog. Phys.* **37**, 1345 (1974); A. C. Roy and N. C. Sil, *J. Phys. B* **12**, 497 (1979) and references therein.
- <sup>11</sup>B. K. Thomas, *Bull. Am. Phys. Soc.* **19**, 1191 (1974). We have learned that while Thomas did not publish his results he reported TDCS for electron-impact ionization of atoms. Also, he made the point that more partial waves are required for TDCS than for total cross sections.
- <sup>12</sup>M. B. Hidalgo, J. H. McGuire, and G. D. Doolen, *J. Phys. B* **5**, L70 (1972).
- <sup>13</sup>J. H. McGuire, M. B. Hidalgo, G. D. Doolen, and J. Nuttall, *Phys. Rev. A* **7**, 973 (1973).
- <sup>14</sup>J. E. Golden and J. H. McGuire, *Phys. Rev. Lett.* **32**, 1218 (1974).

- <sup>15</sup>J. E. Golden and J. H. McGuire, Phys. Rev. A 12, 80 (1975).
- <sup>16</sup>J. E. Golden and J. H. McGuire, J. Phys. B 9, L11 (1976).
- <sup>17</sup>J. E. Golden and J. H. McGuire, Phys. Rev. A 13, 1012 (1976).
- <sup>18</sup>J. E. Golden and J. H. McGuire, Phys. Rev. A 15, 499 (1977).
- <sup>19</sup>A. Tsúji, A. Miyamoto, and H. Narumi, Prog. Theor. Phys. 50, 338 (1973).
- <sup>20</sup>H. Narumi, A. Tsuji, and A. Miyamoto, Prog. Theor. Phys. 54, 740 (1975).
- <sup>21</sup>With the increase in the energy of ejected electrons the number of partial waves increases. Although Narumi *et al.* (Ref. 20) and Golden and McGuire (Ref. 15) have reported that only a few partial waves are needed for the evaluation of total cross sections, accurate evaluation of triple-differential cross sections will involve many more partial waves for large energies of ejected electrons.
- <sup>22</sup>B. K. Thomas and E. Gerjuoy, J. Math. Phys. 12, 1567 (1971).
- <sup>23</sup>A. Nordsieck, Phys. Rev. 93, 785 (1954).
- <sup>24</sup>W. Magnus, F. Oberhettinger, and R. P. Soni, *Formulas and Theorems for the Special Functions of Mathematical Physics* (Springer, New York, 1966), p. 79.
- <sup>25</sup>I. S. Gradshteyn and I. W. Ryzhik, *Table of Integrals, Series, and Products* (Academic, New York, 1965), p. 711.
- <sup>26</sup>Reference 25, p. 1042.
- <sup>27</sup>Reference 24, p. 55.
- <sup>28</sup>M. Abramowitz and I. A. Stegun, *Handbook of Mathematical Functions* (Natl. Bur. Stand. Washington, D. C., 1964), p. 256.
- <sup>29</sup>M. R. H. Rudge, Rev. Mod. Phys. 40, 564 (1968).
- <sup>30</sup>Reference 13, p. 978.
- <sup>31</sup>H. Ehrhardt, K. H. Hesselbacher, K. Jung, M. Schulz, and K. Willmann, J. Phys. B 5, 2107 (1972).
- <sup>32</sup>See N. F. Mott and M. S. W. Massey, *The Theory of Atomic Collisions* (Clarendon, Oxford, 1965), p. 489.
- <sup>33</sup>See, for example, L. Vriens, Physica (Utrecht) 45, 400 (1969).